Stereocontrol of Reactive Encounters Using Polarized Light

Karl-Heinz Gericke,* Christoph Kreher, and Jan Leo Rinnenthal

Institut für Physikalische und Theoretische Chemie, Technische Universität Braunschweig, Hans-Sommer-Strasse 10, D-38106 Braunschweig, Germany

Received: March 21, 1997; In Final Form: May 20, 1997[⊗]

The reaction geometry of selected species can be controlled by using polarized light even in bulk experiments. One reactant A is generated in a photodissociation process. Its spatial distribution is completely described by the anisotropy parameter β. The other molecular reactant B is excited in a specific rovibrational state. Its spatial distribution is given by the *j*- and branch-dependent alignment parameter $A_0^{(2)}$. The unnormalized probability of an attack of A on B under an angle γ is then given by the simple expression $P(\gamma) \propto [1 + {}^1/_5\beta A_0^{(2)} P_2(\cos\gamma)\, P_2(\cos\delta)]$, where δ is the angle between the $\vec{E}$-vectors of the dissociating and of the exciting laser beams. $P_2(x)$ represents the second Legendre polynom. We have studied the reaction of X + HCN → HX + CN with X = H, Cl. The attacking H atom is generated in the photodissociation of CH_3SH at 266 nm, and the chlorine atom is formed in the photolysis of Cl_2 at 355 nm. In both cases the β-parameter is close to −1. In order to align the HCN partner reactant, the first and third vibrational overtone of the CH stretch vibration was excited via the R and P branches. The nascent CN(v=0) product molecules were observed by laser induced fluorescence (LIF). The experimental results prove a preferred linear reaction geometry, i.e. an end-on attack of the X atom on the terminating hydrogen atom of the HCN reactant. However, the angle of acceptance is higher for the Cl + HCN reaction than for the H + HCN one.

I. Introduction

It is well-known that steric effects influence the outcome of a chemical reaction. In organic chemistry special groups are used to protect the molecule from an unwanted spatial attack of a reactant. We have used polarized light to control the reaction geometry of small systems:

$$Cl + HCN(\nu_3,J) \rightarrow HCl + CN \quad (1a)$$

$$H + HCN(\nu_3,J) \rightarrow H_2 + CN \quad (1b)$$

The energy requirements are very similar for both reactions. The Cl + HCN reaction is endothermic (94 kJ/mol)[1] and has a total barrier of 113 kJ/mol.[2] The reaction of H + HCN → H_2 + CN is endothermic by 90 kJ/mol [1] and exhibits a total barrier of 112 ± 3 kJ/mol.[3] Ab initio calculations predict that both Cl + HCN → HCl + CN [4] and H + HCN → H_2 + CN [5] proceed via linear transition states. This is consistent with the experimental observations of rotationally low excited CN product molecules.[6−10]

Several experimental studies have been carried out in order to study the influence of the vibrational mode of the HCN reactant on the reaction. Crim and co-workers[8,11] investigated the reaction dynamics by exciting either four quanta of the CH stretch (004) or a combination mode of three quanta of the CN stretch and two quanta of the CH stretch (302). They concluded that for a H atom attack the CN is formed by a direct abstraction reaction while, in the case of a Cl atom approach, CN is generated via an addition−elimination mechanism in competition with the direct abstraction.

In former studies[9,10,12] we investigated the reactivity of HCN-(ν_1,ν_2,ν_3,J) and reported the state-to-state dynamics of those prepared HCN reactants leading to CN(v,J). A very strong mode specific control of the reaction was achieved; i.e. not the energy but the type of vibrational motion essentially influences the reaction rate. The effect of reactant rotational excitation on both the reaction rate and the CN rotational state distribution was analyzed.

In the present study we investigate the effect of a variation of the reactant approach geometry on the reaction rates. The reactants are aligned by the use of linearly polarized light. Although only two specific reactions of the HCN molecule are analyzed, such experiments in general allow a detailed insight into the stereodynamics of the desired bimolecular reaction. Loesch and co-workers for example also used this technique for similar investigations.[23,24]

II. Experiment

The experimental apparatus has been described in detail previously.[10] In short, translationally excited chlorine atoms were generated from Cl_2 in a pulsed laser photolysis with 20−40 mJ of 355 nm light (Quanta Ray DCR1A). The photolysis produces 98% of the chlorine atoms in the $^2P_{3/2}$ ground spin−orbit state with an anisotropy parameter $\beta = -1 \pm 0.1$.[13] The mean collision energy of the Cl + HCN system is $E_{coll} = 25$ kJ/mol. The precursor of H atoms is methyl mercaptan, dissociated at 266 nm with light generated as the fourth harmonic of a Nd:YAG laser (15 mJ). The photodissociation yields H atoms exclusively with a mean translational energy of 80 kJ/mol. The anisotropy at 266 nm has not been measured, but results at 248 nm ($\beta = -1$)[14] and 274 nm ($\beta = -0.86 \pm 0.05$)[15] suggest that the value is close to −1. The partial pressures were $P(Cl_2) = 8$ Pa and $P(CH_3SH) = P(HCN) = 16$ Pa.

HCN was synthesized by heating a mixture of KCN and stearic acid under vacuum to ≈100 °C. A Nd:YAG laser pumped dye laser (Continuum YG 680, TDL 60, IRP) with a pulse width of typically 7 ns at a bandwidth (fwhm) of 0.07−0.09 cm^{-1} excited the vibrational states of HCN, where different dyes and difference frequency mixing of the dye laser output and the fundamental of the Nd:YAG beam were used to generate turnable IR laser light. A photoacoustic cell served as a probe of the selected HCN transition.

[⊗] Abstract published in *Advance ACS Abstracts,* September 15, 1997.

S1089-5639(97)01015-3 CCC: $14.00

We detected nascent CN products by laser induced fluorescence (LIF) on the $B^2\Sigma^+$ ($v = 0$, $J = 9$) ← $X^2\Sigma^+$ ($v = 0$, $J = 8$) transition at 388 nm using a dye laser (Lambda Physik FL 2002, QUI) pumped by a XeCl excimer laser (Lambda Physik EMG 101 MSC). All LIF spectra were recorded with 2−5 mJ of laser light under saturated conditions. Thus, any influence of aligned CN products on the signal can be neglected. A photomultiplier (THORN-EMI 9781B) monitored the LIF signal perpendicular to the probe beam through f/1 optics and an interference filter (389 ± 10 nm). All lasers were operated at a repetition rate of 10 Hz. The time delay between the photolysis laser, which is in time with the IR/vis excitation laser, and the LIF probe laser was set to 50 ns.

In order to determine the effect of molecular alignment on the reactivity, the polarization of the HCN excitation laser beam with respect to the $\vec{E}$-vector of the photolysis beam was rotated by a $\lambda/2$ plate which was mounted in front of the entrance window of the reaction chamber.

The CN signals of one reaction geometry were averaged by summing over 400 single measurements. This procedure was repeated several times at different polarization schemes in order to minimize the influence of long-term drifts of the laser systems. The accuracy of an intensity measurement was about 1%. It should be mentioned that the use of a photoelastic modulator would further improve the accuracy of the observations because in this case a rotation of the polarization plane can be performed on a shot-to-shot basis.

III. Results and Discussion

The atomic reactants H or Cl are generated in the photodissociation of CH_3SH or Cl_2, respectively. The direction of recoil is determined by the anisotropy parameter β and the ϑ and φ dependence is given by the simple expression[1]

$$\rho_1(\vartheta,\varphi) = \frac{1}{4\pi}(1 + \beta P_2(\cos\vartheta)) \qquad (2)$$

where $P_2(\cos\vartheta) = 3(\cos^2\vartheta - 1)/2$ is the second-order Legendre polynomial. Thus, it always has a cylindrical symmetry. The β parameter ranges from +2 for a pure $\cos^2\vartheta$ distribution to −1 for a pure $\sin^2\vartheta$ distribution; $\beta = 0$ describes a complete isotropic recoil direction. The spatial distribution of the chlorine atom[13] as well as that of the hydrogen atom[14,15] is described by an anisotropy parameter of $b \approx -1$. Thus, the recoiling atom defines the reaction plane, i.e. a $\sin^2\vartheta$ distribution in the laboratory frame (Figure 1).

The transition dipole moment of the molecular reactant, HCN, lies along the internuclear axis, and, therefore, the linearly polarized laser beam selects HCN molecules according to a $\cos^2\theta$ distribution, where θ is measured from the $\vec{E}$-vector of the exciting laser beam. Thus, the initial cylindrical symmetry is broken.

However, it can be shown that the probability for the atom hitting the molecule under an angle γ (where γ is measured from the internuclear HCN axis) depends on the angle δ of the photolysis $\vec{E}$-vector with the excitation $\vec{E}$-vector:[16]

$$P(\gamma) \propto [1 + {}^1/_5\beta A_0^{(2)} P_2(\cos\gamma)\, P_2(\cos\delta)] \qquad (3)$$

where the branch and j dependence is described by the alignment parameter $A_0^{(2)}$.[17]

$$A_0^{(2)} = \begin{Bmatrix} \dfrac{J-1}{2J+1} & \text{P branch} \\ \dfrac{J+2}{2J+1} & \text{R branch} \end{Bmatrix} \qquad (4)$$

The highest alignment can be achieved for the lowest R-branch excitation ($R(0)$: $A_0^{(2)} = 2$). On the other hand, the lowest P-transition, $P(1)$, leads to no alignment of the reactant because the upper excited state is $J = 0$ which has spherical symmetry.

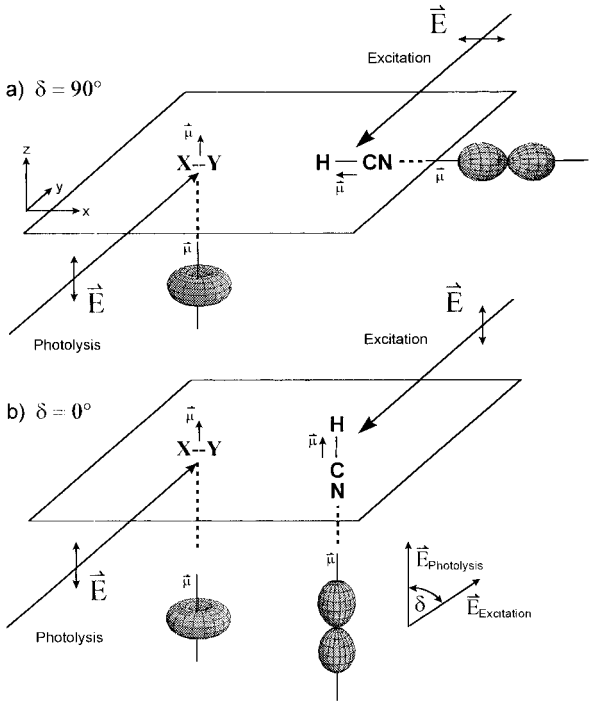

Figure 1. Schematic representation of the spatial alignment of the reactants (Y−X represents Cl−Cl or CH_3S−H). The different polarization of the laser beams leads to different spatial arrangements of the reactants. In the upper part of this figure an end-on attack is preferred (perpendicular polarization between the photolysis and the excitation laser beams). If the $\vec{E}$-vectors are aligned parallel to each other (lower part), then a side-on attack of the atom on the HCN reactant is preferred. For a better visualization polar plots of the spatial distributions are shown: a $\sin^2\vartheta$ distribution for the photolysis products and a $\cos^2\theta$ distribution for the HCN alignment.

A two-dimensional plot of $P(\gamma,\delta)$ for $R(0)$ and $R(8)$ excitation is shown in Figure 2. As one can expect, the largest difference in intensities can be observed for $\delta = 0°$ and $\delta = 90°$. Thus, a change of the alignment of the $\vec{E}$ vectors of the photolyzing and of the exciting laser beams (for HCN) by 90° will induce the largest difference in the product generation, provided there is any stereodynamic effect in the reaction under study. Therefore, $P(\gamma)$ is plotted in a polar diagram for the two experimental situations $\vec{E}_p || \vec{E}_e$ ($\delta = 0°$) and $\vec{E}_p \perp \vec{E}_e$ ($\delta = 90°$). An attack of the approaching atom X on one end of the HCN molecule, i.e. $\gamma = 0$, is preferred for $\delta = 90°$ ($\vec{E}_p \perp \vec{E}_e$). In contrast, a side-on reaction geometry, i.e. $\gamma = 90°$, is preferred for $\delta = 0°$ ($\vec{E}_p || \vec{E}_e$).

Qualitatively this situation is independent of which branch, P or R, and which rotation (with the exception of $P(1)$ excitation) is used to study the reaction dynamics. However, the differences in the reactivity for different polarization schemes are reduced in comparison to $R(0)$ excitation (eqs 3 and 4). The experimental results for the H + HCN(002,J) → H_2 + CN reaction is shown in Figure 3. The HCN molecule is excited to the first overtone of the CH stretch vibration via selected transitions of the P and R branches.

As expected the observed intensity ratio $S = I_\perp/I_{||}$ is 1.0 for the $P(1)$ transition because no aligned HCN is generated. The intensity ratio S is higher for R branch excitation than for P branch excitation, which is also expected qualitatively from eqs 3 and 4. In any case, we observe a value of $S > 1$ which indicates a reaction geometry where the atom preferentially attacks the HCN molecule end-on. Thus, the production of CN molecules is enhanced for collinear collisions of the reactants.

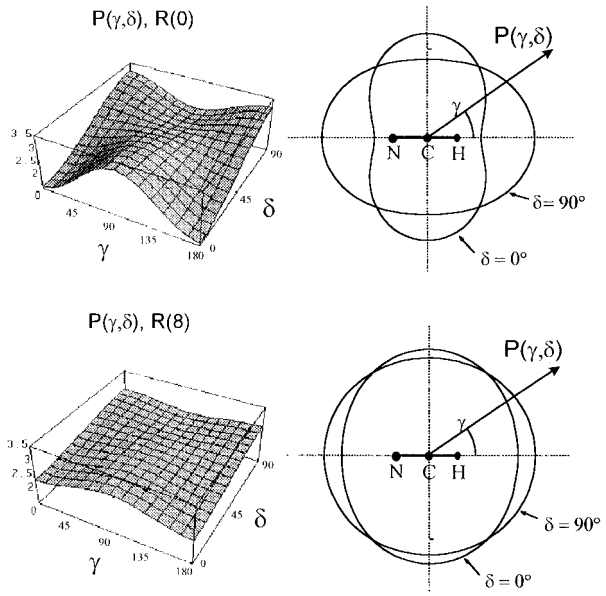

Figure 2. Probability $P(\gamma,\delta)$ as a function of the attack angle and the polarization angle δ, i.e. the angle between the $\vec{E}$-vectors of the photolysis and the excitation laser beams. The polar plots on the right represent the important cases of $\delta = 0°$ (parallel alignment of the $\vec{E}$-vectors) and $\delta = 90°$ (perpendicular alignment). With increasing rotation of the HCN molecule the influence of an alternation of on $P(\gamma,\delta)$ decreases.

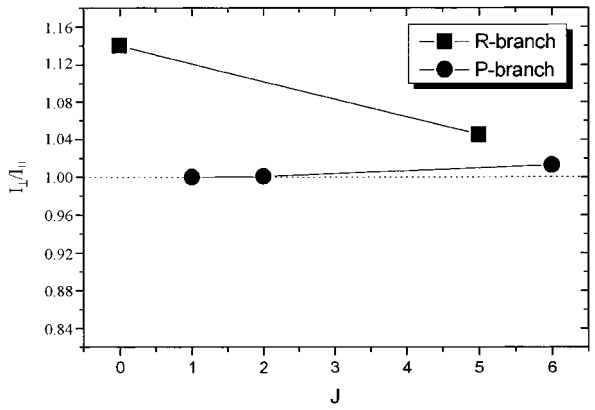

Figure 3. Observed intensity ratio $I_\perp/I_\parallel$ in the reaction of H + HCN-(ν_3=2) → H_2 + CN(υ=0) when the $\vec{E}$-vectors of the photolysis (CH_3S−H) and the HCN excitation laser beams are aligned parallel ($I_\parallel$) or perpendicular ($I_\parallel$) to each other. A value above 1 indicates linear reaction geometry. For low-P-branch excitation, the alignment of the HCN molecule is negligible and no significant deviation from $I_\perp/I_\parallel = 1$ can be expected.

A similar result is obtained when the third overtone of the CH stretch, HCN(004), is excited via the $R(0)$ line ($S = 1.07 \pm 0.03$) or via the $R(8)$ line ($S = 1.09 \pm 0.03$). However, in this experiment the delay time between the excitation laser for generating HCN(004,J) and the CN probe laser was 230 ns, at a total pressure of 50 Pa. We assume that the lower S value, $S = 1.07$, for the HCN(004,J=1) reaction in comparison to $S = 1.14$ for the HCN(002,J=1) reaction is a result of the longer delay time because depolarization effects due to the nuclear spin of HCN have not been considered yet.[18−20]

Precession of the nuclear spin leads to a decrease of the initial molecular alignment. The depolarization is stronger for low J values. For high rotations the total angular momentum F is essentially determined by J, because typical values of I, the nuclear spin, are below $^5/_2$. The influence of the nuclear spin on the polarization measurements can also be neglected, if the time of precession τ_p is long compared to the observation (delay) time τ. On the other hand, if the interaction between J and I is strong, i.e. $\tau_p \ll \tau$, then a time averaged depolarization coefficient can be calculated.

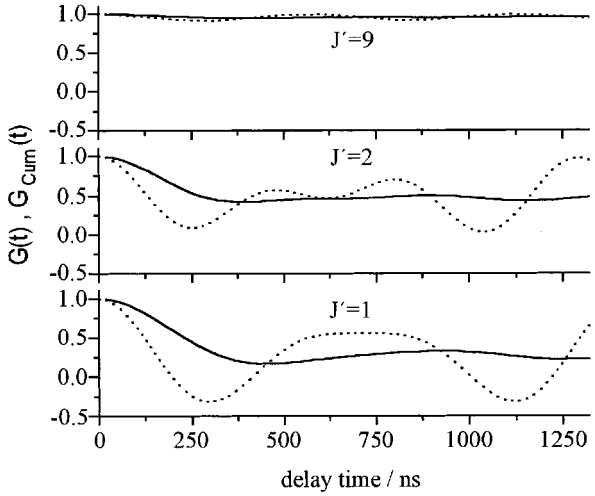

Figure 4. Depolarization $G(t)$ (dashed line) of the HCN reactant ($J' = 1$, 2, and 9) due to quadrupole splitting of the nitrogen atom as a function of time. The solid line represents the accumulated depolarization $G_{Cum}(t)$ which is the relevant quantity for reaction studies. After a few hundred nanoseconds the final values are reached. For $R(0)$ excitation leading to $J' = 1$ the polarization is reduced to 28% of its initial value. For high HCN rotation the depolarization is to be neglected ($\vec{J} \approx \vec{F}$).

For $\tau_P \approx \tau$ the time dependence of the depolarization has to be calculated. In the case of a molecule with one nuclear spin, one obtains

$$A_0^{(2)}(J,t) = G(t)\, A_0^{(2)}(J,t=0) \tag{5}$$

with the time dependent depolarization coefficient $G(t)$:

$$G(t) = \sum_{F,F'} \frac{(2F'+1)(2F+1)}{(2I+1)} \begin{Bmatrix} F' & F & 2 \\ J & J & I \end{Bmatrix}^2 \cos[\Delta E_{FF'} t/\hbar] \tag{6}$$

where $\Delta E_{FF'}$ is the energy separation between two hyperfine levels F and F' of the excited state. In the case of vibronical excitation, the relevant coupling constant of the ground state is a good quantity. According to eq 6 the time averaged depolarization is given by

$$\bar{G}(t) = \sum_{F} \frac{(2F+1)^2}{(2I+1)} \begin{Bmatrix} F & F & 2 \\ J & J & I \end{Bmatrix}^2 \tag{7}$$

In the case of HCN, the H and the N atoms exhibit a nuclear spin ($I_H = {}^1/_2$, $I_N = 1$). However, the coupling of both spins with the nuclear rotation is weak ($C_N = 10.13$ kHz, $C_H = -4.32$ kHz),[21] and, thus, the precession time τ_P is in the upper microsecond range, which is much higher than the relevant time delay τ between excitation and probe beam.

In contrast, the splitting due to the quadrupole of the nitrogen atom is not negligible (eq$Q = -4.71$ MHz),[21] because $\tau_P \approx \tau$, and the time dependence of the depolarization has to be considered. The dotted line in Figure 4 shows the calculated variation of $G(t)$ for the three different rotational states $J' = 1$, 2, and 9, where the calculation has been performed according to ref 22. At a delay time of 230 ns any initial polarization seems to be destroyed. However, for a chemical reaction the cumulative depolarization coefficient

$$G_{Cum}(t') = \frac{1}{t'} \int_0^{t'} G(t)\, dt \tag{8}$$

is important as was pointed out by Orr-Ewing et al.[22] $G_{Cum}(t')$

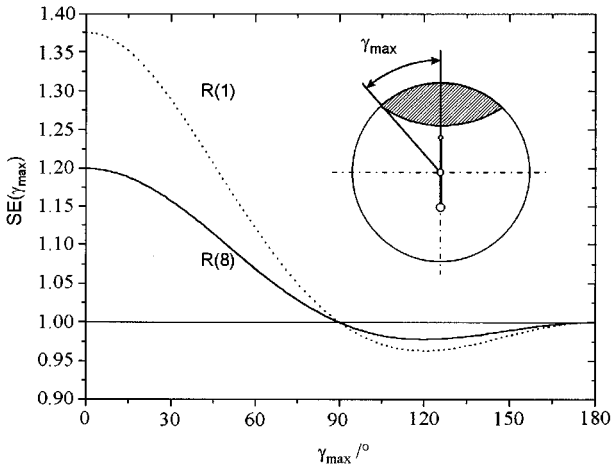

Figure 5. Steric effect SE(γ_{max}) as function of γ_{max}, which defines a cone of acceptance where the reaction takes place. The reaction probability is assumed to be zero for $\gamma > \gamma_{max}$.

is shown in Figure 4 as a solid line. After 350 ns the average depolarization is reached. As a consequence the resulting alignment parameter $A_0^{(2)}$ for $R(0)$ excitation is ($A_0^{(2)}(t) = A_0^{(2)}(t=0)\ G(t) = 2 \times 0.28 = 0.56$) the same as that for $R(8)$ excitation ($A_0^{(2)}(t) = 0.59 \times 0.96 = 0.56$). This is probably the reason why the measured polarization effect for $R(1)$ excitation of HCN(004) ($S = 1.07$) is slightly lower than that for the $R(8)$ line ($S = 1.09$). The reaction of hydrogen atoms with HCN being excited to the first overtone of the CH stretch, HCN(002), was performed at the significantly shorter delay time of 50 ns, where the depolarization due to the quadrupole splitting becomes negligible (Figure 4). Thus, a much higher polarization effect for $R(0)$ excitation in comparison to $R(8)$ excitation can be expected.

The results clearly indicate an essentially linear reaction geometry. In order to gain some insight into how far the attack angle deviates from $\gamma = 0°$ for an exactly linear approach, we assume that the reaction probability does not change as long as the attack angle γ is within a cone of acceptance limited by γ_{max}. Outside of this cone no reaction takes place; i.e. the opacity function $f(\gamma)$ is constant for $0 \le \gamma \le \gamma_{max}$ and vanishes for $\gamma > \gamma_{max}$. The measured signal for a given polarization, i.e. a selected angle δ, is then obtained by integrating eq 3 from $\gamma = 0°$ to $\gamma = \gamma_{max}$. Thus, the steric effect of the reaction is given by

$$\mathrm{SE}(\gamma_{max}) = \frac{\int_0^{\gamma_{max}} P_J(\gamma,\delta=90°)\sin(\gamma)\,\mathrm{d}\gamma}{\int_0^{\gamma_{max}} P_J(\gamma,\delta=0°)\sin(\gamma)\,\mathrm{d}\gamma} \qquad (9)$$

Figure 5 shows SE(γ_{max}) for two rotational transitions. In the reaction H + HCN(ν_3=4,J'=9) → H_2 + CN an intensity ratio of 1.09 ± 0.03 was observed. Since depolarization effects are not very important at this high rotation, the reaction should proceed within a cone of acceptance of $\gamma_{max} \approx 50°$.

When the first CH stretch overtone of HCN is excited via the $R(0)$ line, HCN((ν_3=2,J'=1), then an intensity ratio of 1.14 is observed, which leads to a similar value of γ_{max}. Table 1 gives a summary of the observed intensity ratios and the extracted angle γ_{max} of the cone of acceptance.

The reaction of chlorine atoms with HCN leads to a lower intensity ratio than the H + HCN reaction. According to the cone of acceptance model, the angle γ_{max} must increase to 90° and also some side-on reactions may occur.

Loesch and co-workers obtained similar results when they substituted Li atoms in the reaction Li + HF(v'=1,J'=1) → LIF + H by K atoms.[23,24] The observed steric effect was reduced from SE = 2.2 to SE = 1.19, which is stronger than in our case.

TABLE 1: Observed Steric Effect in the Reaction of R + HCN(ν_3) with R = H, Cl[a]

reaction	transition	E_{av}	$I_\perp/I_\parallel$	γ_{max}, deg
H + HCN(ν_3=2)	$R(0)$	159	1.14	50
H + HCN(ν_3=4)	$R(8)$	232	1.09	55
Cl + HCN(ν_3=2)	$R(8)$	115	1.06	65
Cl + HCN(ν_3=4)	$R(9)$	177	1.00	90

[a] E_{av} is the available energy, and γ_{max} is the cone of acceptance extracted from the observed intensity ratio $I_\perp/I_\parallel$. The error is below 0.03.

In summary, the reaction geometry can be analyzed even in bulk experiments when polarized light is used. At high reactant rotations the dynamic range of the signal intensities at different polarization schemes is fairly low, but sufficient to obtain a quantitative impression of the attack angle. For low rotational states a larger intensity ratio can be expected, provided the influence of depolarization effects can be reduced. This becomes possible when a sufficiently short delay time between preparation of the reactant and probe of the product can be used.

Acknowledgment. We are indebted to Prof. E. A. Reinsch for his significant contribution to eq 3 and for numerous fruitful discussions. We would like to thank Prof. F. J. Comes for material support and stimulating discussions. Financial support of the Deutsche Forschungsgemeinschaft is gratefully acknowledged.

References and Notes

(1) Berkowitz, J.; Ellison, G. B.; Gutman, D. *J. Phys. Chem.* **1994**, *98*, 2744.
(2) Frost, M. J.; Smith, I. W.; Spencer-Smith, R. D. *J. Chem. Soc., Faraday Trans.* **1993**, *89*, 2355.
(3) Schacke, H.; Wagner, H. Gg.; Wolfrum, J. B. *Ber. Bunsen-Ges. Phys. Chem.* **1977**, *81*, 670.
(4) Harding, L. B. *J. Phys. Chem.* **1996**, *100*, 10123.
(5) Bair, R. A.; Dunning, T. H., Jr. *J. Chem. Phys.* **1985**, *82*, 2280.
(6) Lambert, H. M.; Carrington, T.; Filseth, S. V.; Sadowski, C. M. *J. Phys. Chem.* **1993**, *97*, 128.
(7) Johnston, G. W.; Bersohn, R. *J. Chem. Phys.* **1989**, *90*, 7096.
(8) Metz, R. B.; Thoemke, J. D.; Pfeiffer, J. M.; Crim, F. F. *Chem. Phys. Lett.* **1994**, *221*, 347.
(9) Kreher, C.; Theinl, R.; Gericke, K.-H. *J. Chem. Phys.* **1995**, *103*, 8901.
(10) Kreher, C.; Theinl, R.; Gericke, K.-H. *J. Chem. Phys.* **1996,** *104*, 4481.
(11) Pfeiffer, J. M.; Metz, R. B.; Thoemke, J. D.; Woods, E., III; Crim, F. F. *J. Chem. Phys.* **1996**, *104*, 4490.
(12) Kreher, C.; Rinnenthal, J. L.; Gericke, K.-H. To be published.
(13) Matsumi, Y.; Tonokura, K.; Kawasaki, M. *J. Chem. Phys.* **1992**, *97*, 1065.
(14) Jensen, E.; Keller, J. S.; Waschewsky, G. C. G.; Stevens, J. E.; Graham, R. L. *J. Chem. Phys.* **1993**, *98*, 2882.
(15) Wilson, S. H. S.; Ashfold, M. N. R.; Dixon, R. N. *J. Chem. Phys.* **1994**, *101*, 7538.
(16) Reinsch, E.; Gericke, K.-H.; Kreher, C. To be published.
(17) Zare, R. N. *Ber. Bunsen-Ges. Phys. Chem.* **1982**, *86*, 422.
(18) Altkorn, R.; Zare, R. N. *Mol. Phy.* **1985**, *55*, 1.
(19) Greene, C. H.; Zare, R. N. *Annu. Rev. Phys. Chem.* **1982**, *33*, 119.
(20) Orr-Ewing, A. J.; Zare, R. N. *Annu. Rev. Phys. Chem.* **1994**, *45*, 315.
(21) Lovas, F. J. *J. Phys. Chem. Ref. Data* **1978**, *7*, 1445.
(22) Orr-Ewing, A. J.; Simpson, W. R.; Rakitzis, T. P.; Zare, R. N. *Is. J. Chem.* **1994**, *34*, 95. Zare, R. N. *Angular Momentum. Understanding Spatial Aspects in Chemistry and Physics*; Wiley-Interscience: New York, 1988.
(23) Hoffmeister, M.; Schleysing, R.; Loesch, H. J. *J. Phys. Chem.* **1987**, *91*, 5441.
(24) Loesch, H. J.; Stenzel, E.; Wüstenbecker, B. *J. Chem. Phys.* **1991**, *95*, 3841.